



HAL
open science

Modelling differential scanning calorimetry curves of precipitation in Al-Cu-Mg

Emmanuel Hersent, Julian Haworth Driver, David Piot

► **To cite this version:**

Emmanuel Hersent, Julian Haworth Driver, David Piot. Modelling differential scanning calorimetry curves of precipitation in Al-Cu-Mg. *Scripta Materialia*, 2010, 62 (7), pp.455-457. 10.1016/j.scriptamat.2009.12.009 . hal-00854051

HAL Id: hal-00854051

<https://hal.science/hal-00854051v1>

Submitted on 17 Aug 2022

HAL is a multi-disciplinary open access archive for the deposit and dissemination of scientific research documents, whether they are published or not. The documents may come from teaching and research institutions in France or abroad, or from public or private research centers.

L'archive ouverte pluridisciplinaire **HAL**, est destinée au dépôt et à la diffusion de documents scientifiques de niveau recherche, publiés ou non, émanant des établissements d'enseignement et de recherche français ou étrangers, des laboratoires publics ou privés.



Distributed under a Creative Commons Attribution - NonCommercial 4.0 International License

Modelling differential scanning calorimetry curves of precipitation in Al–Cu–Mg

E. Hersent, J.H. Driver* and D. Piot

Materials Centre and CNRS UMR 5146, Ecole des Mines de Saint Etienne, 158 Cours Fauriel, 42023 Saint Etienne, France

The heat flux during a differential scanning calorimetry (DSC) experiment of a precipitation reaction is expressed analytically as a function of the interfacial energy, the solid solution composition and the precipitate fraction. Using a physically based model of nucleation, growth and dissolution, the respective contributions of these terms are compared for the case of S phase precipitation in AA2024 (Al–4% Cu–2% Mg). Good overall agreement is obtained for the experimental and simulated DSC curves if the interfacial energy is tuned correctly.

Keywords: Differential scanning calorimetry (DSC); Aluminium alloys; Phase transformation kinetics; Simulation; Thermodynamics

Differential scanning calorimetry (DSC) is a popular technique with which to study the thermodynamics and kinetics of phase changes in materials. It is particularly useful for precipitation reactions in light alloys used for structural applications, where successive solid-state reactions of precipitation and dissolution can be analysed at increasing temperatures (e.g. [1]). The nucleation or dissolution of a phase in a DSC experiment is characterized by a heat flow peak over the reaction temperature range, and the peak area gives a semi-quantitative evaluation of the phase quantities involved in the reaction. The area under the peak is proportional to the molar enthalpy of precipitation, and the displacement of the peak with heating rates can be linked to the activation energy.

Over the last 20 years, modelling simulations of precipitation have made significant progress, in particular by using the numerical framework developed by Wagner and Kampmann [2]. This method can be used to simulate the evolution of the precipitate radius distribution during any heat treatment and is now an established tool for predicting the evolution of homogeneously nucleated particles in both simple and commercial alloys. An important application of this model is the simulation of precipitation in age-hardening aluminium alloys during welding [3].

Modelling DSC curves from the basic physical principles of precipitation/dissolution has rarely been at-

tempted, perhaps because it requires a demanding accuracy of both the thermodynamics and kinetics of transformations. DSC curves for precipitate dissolution have been simulated, e.g. by Chen et al. [4], but to our knowledge only Khan and Starink [5] have published simulated DSC curves for precipitation and dissolution in Al alloys. However, their analysis seems to have some deficiencies: the units of their Figure 3 in W g^{-1} do not correspond to their equation for $\Delta H \times dV_s/dt$ in kJ mol^{-1} , and more surprisingly the heating rate does not appear to influence the DSC curves.

In light of this, it seems that a proper model for the DSC precipitation experiment is needed, and that is the goal of this article. We will first establish an analytical expression of the heat flux in a simple two-phase reaction (precipitation and dissolution). This will be applied to the case of S (Al_2CuMg) phase precipitation in AA2024 (Al–4% Cu–2% Mg) by simulating the heat flux due to S phase precipitation and dissolution in a DSC experiment.

We consider a system where the precipitates appear from a supersaturated solid solution. We suppose that the precipitates form a unique phase and that their interfacial energy γ is independent of the precipitate–matrix orientation relation. The total Gibbs energy is:

$$G = g_{ss}^v V_{ss} + \left(\sum_{\text{precipitates}} V_p \right) + \Delta g_p^v \sum_{\text{precipitates}} V_p + \gamma \times \sum_{\text{precipitates}} A_p \quad (1)$$

* Corresponding author. E-mail: driver@emse.fr

where g_{ss}^v is the Gibbs energy per volume of the solid solution, Δg_p^v is the difference of Gibbs energy per volume between the precipitates and the solid solution, V_{ss} is the volume of the solid solution, and V_p and A_p are the volume and surface area of one precipitate. The total Gibbs energy per unit volume of the system G_{sys}^v is:

$$G_{sys}^v = g_{ss}^v + \Delta g_p^v \cdot f_v + \gamma \cdot \frac{A}{V_{sys}} \quad (2)$$

where f_v is the volume fraction of the precipitates and A is the total surface developed by the precipitates ($\sum_{\text{precipitates}} A_p$). The quantities which are referenced in thermodynamics database are quantities per mole, not per volume, and are obtained by dividing Eq. (2) by the molar volume. For DSC one also divides by ρ , the weight per unit volume of the alloy, to give the total Gibbs energy per unit mass:

$$G_{sys}^w = \frac{1}{\rho} \left(\frac{g_{ss}^m}{V_{ss}^m} + \frac{\Delta g_p^m}{V_p^m} \cdot f_v + \gamma \cdot \frac{A}{V_{sys}} \right) \quad (3)$$

In DSC experiments, the heat flow of a sample is not measured absolutely but relative to a reference which does not undergo a phase change in the temperature range. For aluminium alloys, the chosen reference is usually high-purity aluminium. The heat flux per gram of a sample $\dot{q} = \frac{d}{dt}(H - H^{REF})$ can be derived from Eq. (3) with the help of the standard relations $H = G + TS$ and $S = -\left. \frac{\partial G}{\partial T} \right|_{P, \text{ fixed composition}}$:

$$\dot{q} = \frac{d}{dt} \left(G_{sys}^w - T \left. \frac{\partial G_{sys}^w}{\partial T} \right|_{P, \text{ fixed composition}} \right) - \frac{dH^{REF}}{dt} \quad (4)$$

H^{REF} can be easily calculated from the molar Gibbs energy of aluminium given in standard databases such as that in Ref. [6]. The main alloying elements of AA2024 are copper and magnesium, so the Gibbs molar enthalpy g_{ss}^m can be approximated by:

$$g_{ss}^m = x_{Al} \mu_{ss}^{Al} + x_{Cu} \mu_{ss}^{Cu} + x_{Mg} \mu_{ss}^{Mg} \quad (5)$$

It has been demonstrated for aluminium alloys that the regular solid solution model is sufficient to accurately calculate phase diagrams in the aluminium-rich corner [7]. The molar Gibbs energies of aluminium, copper and magnesium are thus given by:

$$\begin{aligned} \mu_{ss}^{Al} &= \mu_{PURE}^{Al} + RT \ln x_{Al} \\ \mu_{ss}^{Cu} &= \mu_{PURE}^{Cu} + RT \ln x_{Cu} + \Omega_{Al-Cu}(T) * (x_{Al})^2 \\ \mu_{ss}^{Mg} &= \mu_{PURE}^{Mg} + RT \ln x_{Mg} + \Omega_{Al-Mg}(T) * (x_{Al})^2 \end{aligned} \quad (6)$$

When the composition of each phase is fixed, the reaction rate is zero, and the volume fraction and precipitate surface area are constant. As shown in the Appendix, the final expression of the heat flux \dot{q} can then be written:

$$\dot{q} = \frac{d}{dt} \left(\frac{h_{ss}^m - h_{Al}^m}{V_m} + \frac{\Delta h_p^m}{V_p} \cdot f_v + \left(\gamma - \left. \frac{\partial \gamma}{\partial T} \right|_P \right) \cdot \frac{A}{V_{sys}} \right) \quad (7)$$

This differs from the equation used by Khan and Starink [5], $\dot{q} = \Delta H * \frac{d}{dt}(f_v)$, by a term for the heat evolution due to compositional change in the solid solution (and which needs to be evaluated).

This expression was used to simulate the contribution of S phase to the heat flux during a DSC experiment on AA2024. Following Khan et al. [8], we assume, for simplicity, that the 2024 aluminium alloy is a pseudo-binary with the concentrations of copper and magnesium in the Al-rich phase in constant ratio to each other during the entire process. To simulate S precipitation, the numerical framework for nucleation, growth and dissolution of particles described by Myhr and Grong [9] has been applied to obtain the theoretical particle size evolutions with time and temperature. This is a physically based model of particle nucleation and growth for different particle size classes.

The model obviously requires a number of parameters to be known with good accuracy. The most critical of these is the interfacial energy γ . One solution adopted by Kamp et al. [10] consists of calibrating the interfacial energy with the evolution of the volume fraction measured by small angle X-ray scattering during reversion treatments. For the present alloy it is necessary to introduce a temperature dependence to achieve a nearly peak strength independent of temperature during isothermal treatments [8]. For the precipitation stage we use a relation similar to that of Khan and Starink [5] as given in Table 1, for which γ decreases with temperature (from about 0.08–0.05 J m⁻² over the temperature of interest).

The shape of the S particles was taken to be a rod with a constant aspect ratio [8]. Other parameters, such as the diffusion coefficient of Cu in Al, are given in the table. The average atomic volume of S phase (Al₂CuMg) is nearly the same as that of the face-centred cubic Al matrix [11], so one can take $V_p^m \approx 4 * V_m$. Also, in a typical 2024 aluminium alloy, the Al molar fraction is about 0.95, so x_{Al} is approximated by unity in the following. The values of $\Omega_{Al-Cu}(T)$ and $\Omega_{Al-Mg}(T)$ are listed in Table 1.

Although the standard composition of the industrial alloy is about 4.2 wt.% Cu, approximately 0.8% Cu is tied up in the intermetallic particles (stable to high temperatures) and therefore does not participate in the reactions: the active composition was taken as 3.4 wt.% Cu.

DSC curves were simulated assuming a quenched and room tempered alloy (i.e. containing GP zones of average radius 0.6 nm and number density 2×10^{25} per m³). For a standard heating rate of 20 °C min⁻¹ the simulated DSC curve is given in Figure 1, together with the contributions of each heat flux term (in dotted lines). This DSC curve first exhibits a small endothermic reaction at 150–250 °C, usually taken to be GP zone dissolution. There is then a large exothermic peak at 250–320 °C due to S phase precipitation and finally a long S phase dissolution trough at 320–470 °C. It is also clear that the volume en-

Table 1. Summary of the input data used in the model.

$\Omega_{Al-Cu}(T)$ (J mol ⁻¹)	-13760
$\Omega_{Al-Mg}(T)$ (J mol ⁻¹)	6821–3.077T
Δh_p^m (kJ mol ⁻¹)	75 kJ mol ⁻¹ [5]
γ (J m ⁻²)	-0.10985 + 8.3074 × 10 ⁻⁴ T - 8.7143 × 10 ⁻⁷ T ²
ρ (kg m ⁻³)	2.77 × 10 ³
D_{Cu}^{Al} (m ² s ⁻¹)	6.47 · 10 ⁵ e ^{$\frac{-135 \text{ kJ mol}^{-1}}{RT}$}

$\Omega_{Al-i}(T)$ is the sum of the Redlich–Kister coefficients of the binary Al–i system.

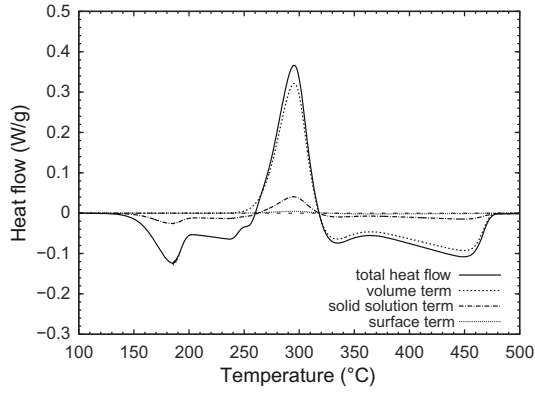


Figure 1. DSC model prediction of the different terms involved in the heat flow during heating AA2024 at 20 °C min⁻¹.

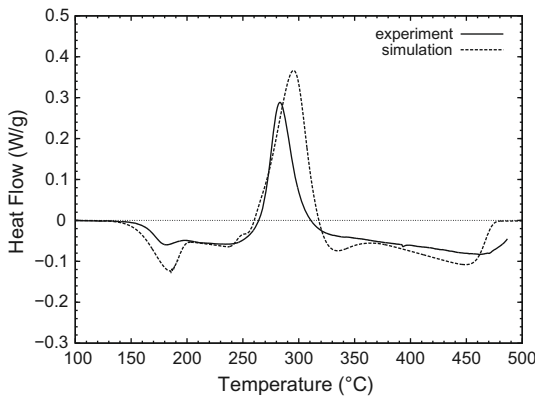


Figure 2. DSC model prediction of the heat flow compared with an experimental scan measured for a heating rate of 20 °C min⁻¹.

thalpy term (ΔH) contributes about 90% of the heat flux, with most of the remaining 10% due the solid solution term. The contribution of the interface energy is very small, which is not surprising since only a very small fraction of the atoms is involved in the interface. Consequently, the volume enthalpy term can be taken as a first-order approximation of the heat flux and the peak area could then be used to determine the volume fraction of the precipitating S phase.

The simulated and experimental heat flow curves are given in Figure 2. The experimental DSC curve was obtained on a standard AA2024 alloy (T 351 condition) using a SETARAM model DSC 131; it is very similar to previous published DSC plots of this alloy [12]. It can be seen that the simulated DSC curve is very close to the experimental one, with the peaks and troughs of similar amplitude over the same temperature ranges.

This type of DSC simulation can in fact be considered as a test or estimation of the interfacial energy. The reaction enthalpy for precipitate dissolution is given, to first order, by the area under the high-temperature dissolution curve. The other thermodynamic parameters are usually known or can be estimated as done here (given that the interfacial energies have little influence on the peak amplitudes). However, the kinetics, or the temperatures of the heat flow peaks in a DSC experiment, are then strongly dependent on the diffusion coefficients and the interfacial energies. If the diffusion coefficients are known it should be possible to deduce the interface energies by a fitting

procedure from the experimental DSC curves and this type of model simulation. The strong influence of the interfacial energy on the DSC simulation has been checked by changing its value by 10%: this produces a change in peak temperature of about 100 °C.

In conclusion, the expression for the heat flux during a DSC experiment involving a two-phase reaction has been refined to include the heat evolution due to compositional change in the solid solution. It has been applied to the formation and dissolution of S precipitates in a 2024 aluminium alloy and shown to give good agreement with experimental DSC curves. Nevertheless, it is shown that, to first order, the expression of the heat flux can be approximated by the standard term $\frac{V_m}{V_p^m} \frac{\Delta H}{M_{Al}} \frac{df_v}{dt}$. In a wider context, it is suggested that the interfacial energies can be deduced from DSC curves of precipitation reactions (assuming that the phases etc. are known) by comparison with the temperature dependence of curves simulated using physically based models.

Appendix

The goal of the appendix is to show that the enthalpy of $\frac{\Delta g_p^m}{V_p^m} f_v$ can be written as $\frac{\Delta h_p^m}{V_p^m} f_v$.

$$\begin{aligned} \frac{\Delta g_p^m}{V_p^m} f_v - T \frac{\partial}{\partial T} \left(\frac{\Delta g_p^m}{V_p^m} f_v \right) \Big|_{P, \text{ fixed composition}} \\ = \frac{\Delta g_p^m}{V_p^m} f_v - T \frac{f_v}{V_p^m} \frac{\partial}{\partial T} \left(\Delta g_p^m \right) \Big|_{P, \text{ fixed composition}} \end{aligned}$$

because at this fixed composition, there is no exchange of matter between phases, so the volume fraction is fixed and independent of temperature. The latter equation can be simplified to:

$$\frac{f_v}{V_p^m} \left(\Delta g_p^m - T \frac{\partial}{\partial T} (\Delta g_p^m) \right) = \frac{f_v}{V_p^m} \Delta h_p^m$$

A similar reasoning can be applied to the term $\gamma A/V_{\text{sys}}$.

- [1] M.J. Starink, *Int. Mater. Rev.* 49 (2004) 191.
- [2] R. Wagner, R. Kampmann, in: R.W. Cahn (Eds.), *Materials Science and Technology – A Comprehensive Treatment*, VCH, Weinheim, 1991, pp. 213–303.
- [3] O.R. Myhr, Ø. Grong, H.J. Fjær, C.D. Mariora, *Acta Mater.* 52 (2004) 4997.
- [4] S.P. Chen, M.S. Vossenbergh, F.J. Vermolen, J. van de Langkruis, S. van der Zwaag, *Mater. Sci. Eng. A* 272 (1999) 250.
- [5] I.N. Khan, M.J. Starink, *Mater. Sci. Technol.* 24 (2008) 1403.
- [6] A.T. Dinsdale, *Calphad* 15 (1991) 317.
- [7] C. Sigli, L. Maenner, C. Stzur, R. Shahani, in: T. Sato, S. Kumai, T. Kobayashi, Y. Murakami, *Aluminium Alloys: Their Physical and Mechanical Properties (ICAA6)*, The Japan Institute of Light Metals, Toyohashi, 1998, pp. 87–98.
- [8] I.N. Khan, M.J. Starink, J.L. Yan, *Mater. Sci. Eng. A* 472 (2008) 66.
- [9] O.R. Myhr, Ø. Grong, *Acta Mater.* 48 (2000) 1605.
- [10] N. Kamp, A. Sullivan, J.D. Robson, *Mater. Sci. Eng. A* 466 (2007) 246.
- [11] H. Perltz, A. Westgren, *Ark. Chem. Miner. Geol.* 16B (1943) 13.
- [12] M.J. Starink, N. Gao, L. Davin, J. Yan, A. Cerezo, *Philos. Mag.* 85 (2005) 1395.